Supporting Information

One-pot assembly of metal/organic-acid sites on amine-functionalized ligands of MOFs for photocatalytic hydrogen peroxide splitting

Lei Qin,[a] Zhaowen Li, [a] Qiong Hu, [a] Zehai Xu, [a] Xinwen Guo [b] and Guoliang Zhang*[a]

[a] *Institute of Oceanic and Environmental Chemical Engineering, State Key Lab Breeding Base of Green Chemical Synthesis Technology, Zhejiang University of Technology, Hangzhou 310014, China*

[b] *State Key Laboratory of Fine Chemicals, Department of Catalysis Chemistry and Engineering, Dalian University of Technology, Dalian 116012, China*

Tel/Fax: 86-571-88320863; E-mail: guoliangz@zjut.edu.cn

EXPERIMENTAL SECTION

Chemicals. All reagents were purchased commercially and used without further purification. All chemicals, such as terephthalic acid ($HOOCC_6H_4COOH$, 99 %), 2-amino terephthalic acid (HO_2C-$C_6H_3NH_2$-CO_2H), N,N-dimethylformamide ($(CH_3)_2NCHO$), aluminum chloride hexahydrate ($AlCl_3$ $6H_2O$), aluminum nitrate nonahydrate ($Al(NO_3)_3$ $9H_2O$), aqueous hydrofluoric acid (HF, 40 %) , ethanol amine, ferric nitrate ($Fe(NO_3)_3 \cdot 9H_2O$), hydrochloric acid (HCl, 35 wt. %), ethanol, benzene (C_6H_6, 99.5%), acetonitrile (MeCN, 99%), hydrogen peroxide (H_2O_2, 30%) and dichloromethane (CH_2Cl_2, 99.5%) were of analytical grade and were purchased from Sinopharm chemical Reagent Co, China. All experiment solutions were prepared from deionized water manufactured by a self-made RO-EDI system, in which ion concentration was analyzed and controlled by IRIS Intrepid ICP and Metrohm 861Compact IC.

Synthesis of NH_2-MIL-101(Al). The NH_2-MIL-101(Al) was synthesized by means of a solvothermal treatment involving N, N-dimethylformamide (DMF) as solvent. Starting reactants were aluminum chloride hexahydrate, 2-amino terephthalic acid and N, N-dimethylformamide. The reactants were placed into a 50 mL Teflon-lined autoclave and heated for 72 h at 403 K in an oven under static conditions. The resulting yellow powders were isolated under centrifugation and washed with acetone. To remove organic species trapped within the pores, the samples were stirred in methanol overnight and dried at 353 K after washed by methanol for several times.

Synthesis of NH_2-MIL-53(Al). In a typical synthesis, aluminum chloride hexahydrate and 2-amino terephthalic acid were dissolved in a certain amount of N,N-dimethylformamide, while the volume of solvent was kept constant at 30 mL. The mixture was introduced into a 50 mL Teflon-lined steel autoclave and placed in an oven at 423 K for 24h under static conditions. After

cooling down, the yellow solid products were isolated by centrifugation. Then the products were activated in DMF for 5h in a Teflon-lined steel autoclave in order to remove the remaining water molecules or unreacted ligands trapped in the pores. Finally, the product was isolated by repeated centrifugation and washed with dimethyl ketone for 3 times. The resulting solids were all white and dried overnight at 353 K.

Synthesis of MIL-53(Al). The synthesis was carried out under mild hydrothermal conditions using aluminum nitrate nonahydrate, 1,4-benzenedicarboxylic acid and deionized water. The reaction was performed in Teflon-lined stainless steel under autogenous pressure for 3 days at 493 K. The molar composition of the starting gels was 1 Al (1.30 g): 0.5 BDC (0.288 g): 80 H_2O. The white product was centrifugated and cleaned with deionized water and dried at 353 K.

Synthesis of CFH@Al-MOFs. In a typical synthesis, NH_2- MIL-101(Al), NH_2-MIL-53(Al) or MIL-53(Al) was activated at 353 K under vacuum, and 1 g of which was dispersed on glass plate. The deionized water solution containing $Fe(NO_3)_3$ (0.007 mol L^{-1}) and a certain amount of critic acid (The molar composition of the starting gels was 1 Fe^{3+}: 1.5 CA) were sprayed on the Al-MOFs under certain temperature. The obtained powders were washed with distilled water for three times and dried under 353 K to acquire CFH@NH_2-MIL-101(Al). Then the as-synthesized samples were treated in a stream of air at 473 K for 4h to yield the CFH@NH_2-MIL-101(Al), CFH@NH_2-MIL-53(Al) and CFH@MIL-53(Al) subsequently.

Synthesis of FH@Al-MOFs. The pathway used to fabricate FH@MOFs was similar to the synthesis of CFH@Al-MOFs but without CA in the sparing solution. The final samples were marked as FH@ MIL-53(Al), FH@NH_2-MIL-53(Al) and FH@MIL-53(Al), respectively.

Synthesis of CFH@ P25, Clay, and meso NH_2-SiO_2 sphere. The route used to fabricate

CFH@ P25, Clay, and meso NH_2-SiO_2 is similar to the synthesis of CFH@Al-MOFs.

Characterization. The surface morphology of the prepared samples was evaluated by Hitachi JEM-1200EX transmission electron microscopy (Hitachi, Japan) and JEM-2100 transmission electron microscopy (Jeol, Japan) and Tecnai G2 F30 S-Twin high resolution transmission electron microscopy (Philips-FEI, Holland). Fourier Transform Infrared (FTIR) spectrophotometers of the samples were recorded by the KBr disk technique with Nicole 6700 Fourier transform infrared spectrometer (Thermo, USA). The X-ray diffraction (XRD) of the nanocomposites was determined by X'Pert PRO X-ray diffractometer (PNAlytical, Cu Kα radiation). Nitrogen adsorption-desorption isotherms were obtained by an ASAP 2020 surface area and porosity analyzer (Micromeritics, USA) at 77 K. Energy dispersive spectroscopy (Hitachi, S-3700N, Japan) was taken for the composition detection of different samples. The X-ray photoelectron spectroscopy (XPS) experiments were carried out on a RBD upgraded PHI-5000C ESCA system (Perkin Elmer) with Mg Kα radiation (hν=1253.6eV), and binding energies were calibrated by using the containment carbon (C1s=284.6eV). The compositional analysis of catalysts was performed by ICP-AES in an Optima 2000 instrument (PerkinElmer, USA) after the samples microwave digestion in acid solution.

Catalytic experiments. The generation of OH radicals was analyzed by the direct hydroxylation of benzene to phenol. The experiments were initiated by adding 6 mL MeCN, 4.0 mL H_2O_2, 1.8 mL benzene and 0.01 g prepared catalysts under visible light irradiation (200 W halogen lamp, emission wavelength: 350-450 nm) and stirred for 5 h at 333 K. 0.5 mL of suspension was sampled and filtered through microfiltration membrane to separate catalysts, and which was then extracted by CH_2Cl_2. The mixture was analyzed by HPLC (Shimadzu, GC2014).

Table S1 Corresponding EDS results of the different samples

Sample	Element	Atom %	Element WT %
CFH@MIL-53(Al)	C-K	58.12	48.77
	O-K	36.15	40.40
	Al-K	5.73	10.80
	Fe-K	0.01	0.004
CFH@NH_2-MIL-53(Al)	C-K	55.14	45.14
	O-K	37.75	41.17
	Al-K	6.79	12.40
	Fe-K	0.31	1.20
CFH@NH_2-MIL-101(Al)	C-K	60.25	50.84
	O-K	34.78	39.09
	Al-K	4.65	8.81
	Fe-K	0.32	1.25

Table S2 Compositions of Fe nanoclusters for sample [Fe-O-C]@NH_2-MOF

Fe nanoclusters composition	CFH@NH_2-MIL-53	CFH@NH_2-MIL-101
Fe (wt. %)	0.550	1.66
C (wt. %)	0.0868	0.260
O (wt. %)	0.329	0.982

Table S3 Surface area, textural data and metal compositions for different samples.

Sample	S_{BET} (m^3/g)[a]	$S_{Langmuir}$ (m^3/g)[b]	V_{meso}(cm^3/g)[c]	Fe loaded (mg/g)[d]
MIL-53(Al)	1008.1	1436.1	0.35	-
CFH@MIL-53(Al)	920.7	1211.3	0.32	0.16
NH_2-MIL-53(Al)	961.7	1169.2	0.24	-
CFH@NH_2-MIL-53(Al)	601.2	839.2	0.19	5.50
NH_2-MIL-101(Al)	1240.4	1810.7	0.69	-
CFH@NH_2-MIL-101(Al)	960.8	1210.7	0.36	16.60

[a] S_{BET} is the BET specific surface area.

[b] $S_{Langmuir}$ is the Langmuir specific surface area.

[c] Vmeso is the specific mesopore volume obtained from the BJH cumulative specific adsorption volume of pores of 1.70-300.00 nm in diameter.

[d] Analysis of ICP–MS.

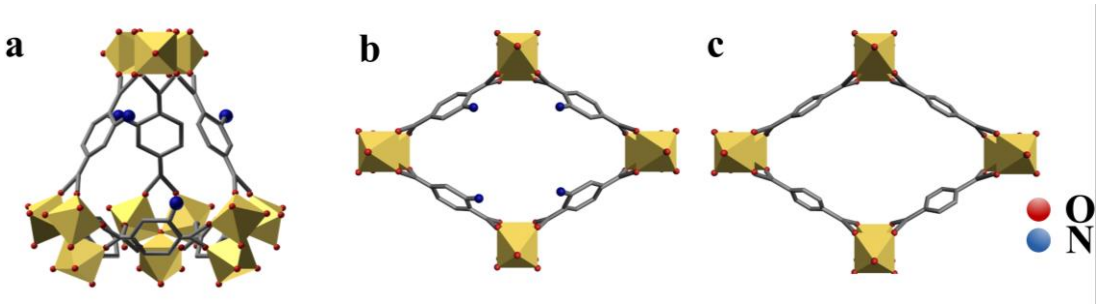

Figure S1 Structure of NH_2- MIL-101 (a), NH_2- MIL-53 (b), and MIL-53 (c).

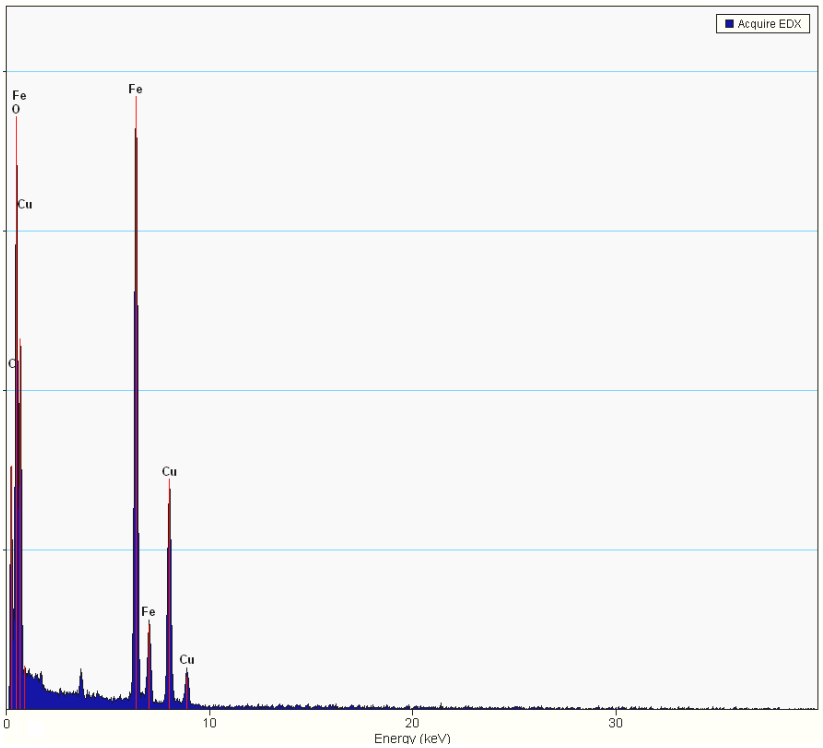

Figure S2 EDS analysis of Fe based nanoclusters

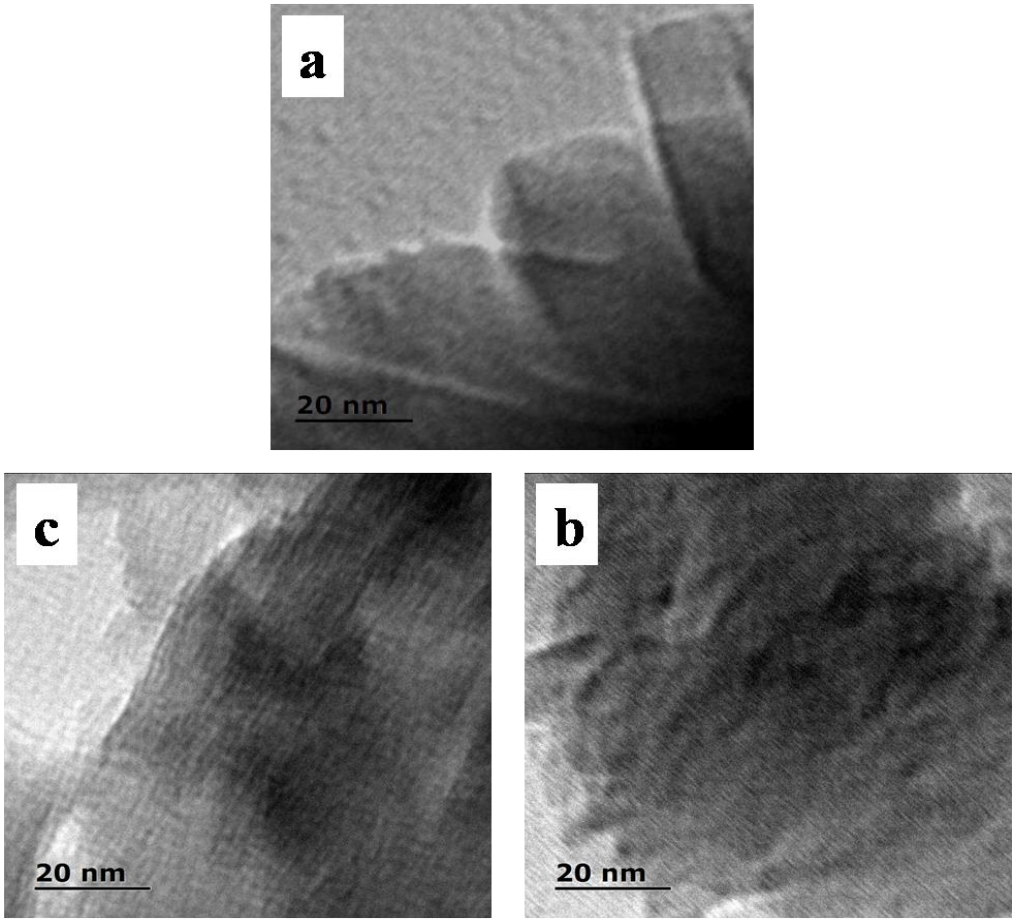

Figure S3 HRTEM images of CFH@MIL-53 (a); CFH@NH_2-MIL-53 (b), and CFH@NH_2-MIL-101 (c).

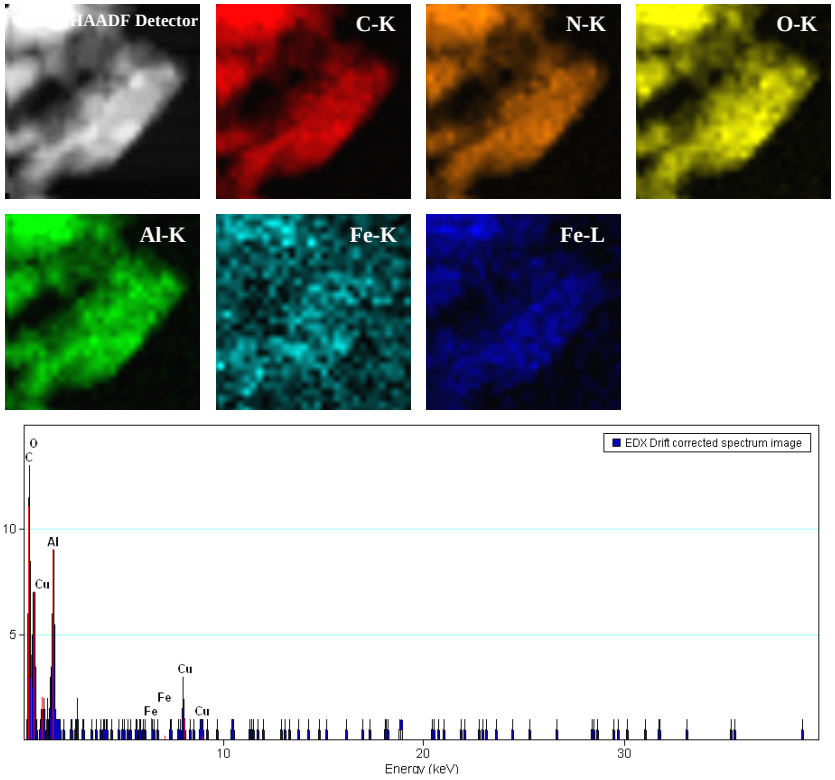

(a)

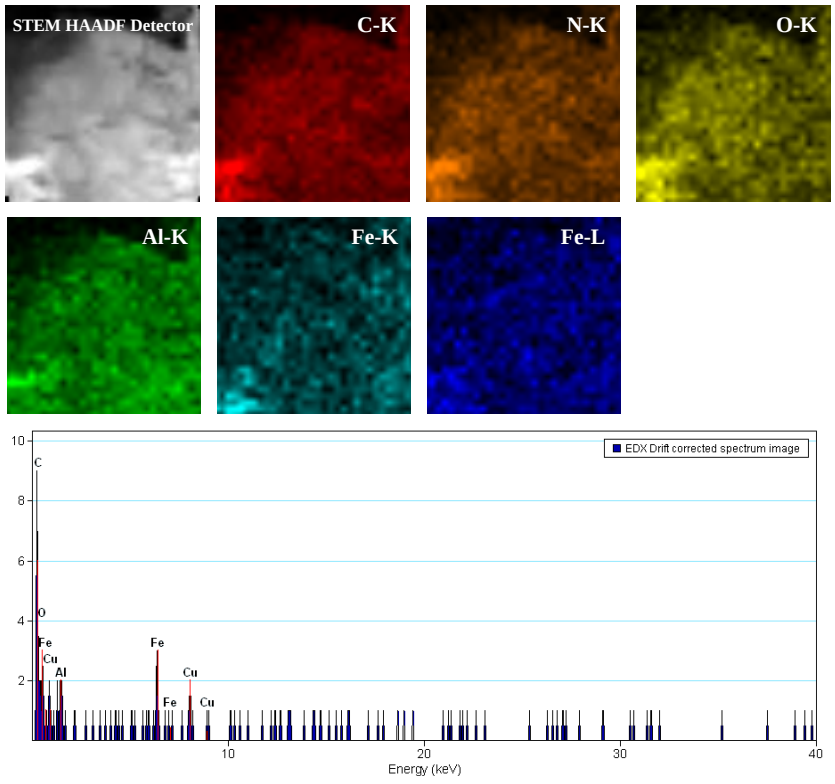

(b)

Figure S4 STEM-HAADF image of as synthesized [Fe-O-C]@NH_2-MIL-53 (a) and [Fe-O-C]@NH_2-MIL-101 (b), and TEM elemental mapping of C, N, Al, O and Fe.

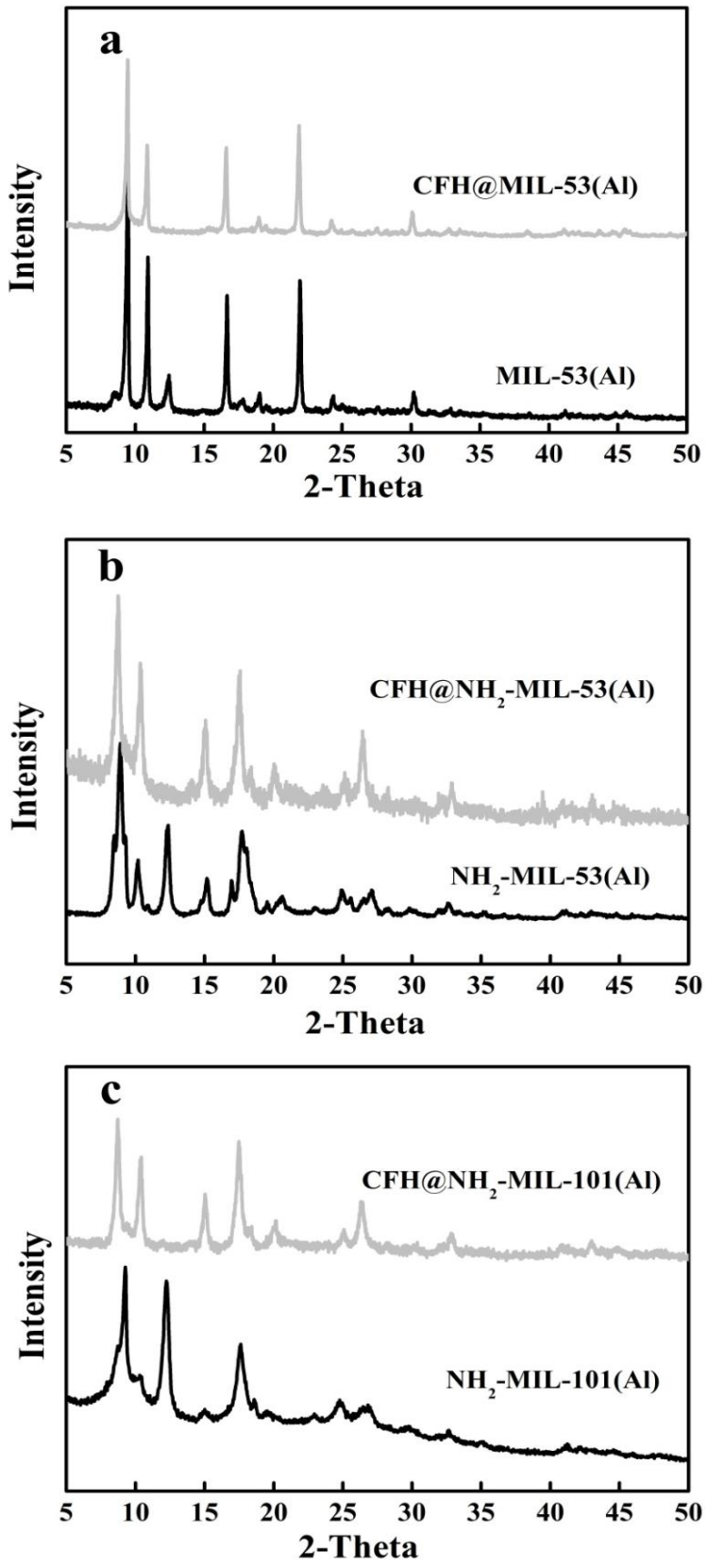

Figure S5 XRD spectrum of the different samples.

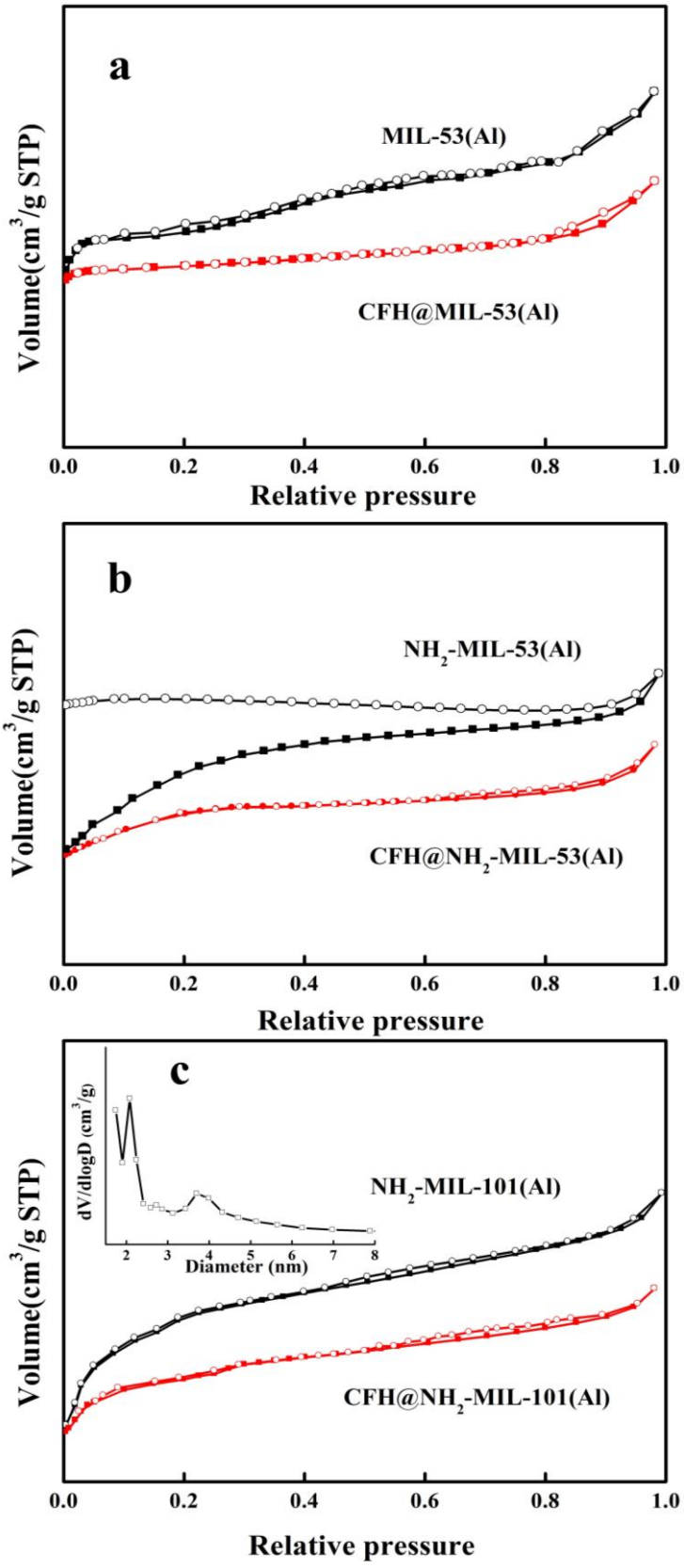

Figure S6 Nitrogen adsorption/desorption isotherms and of different samples.

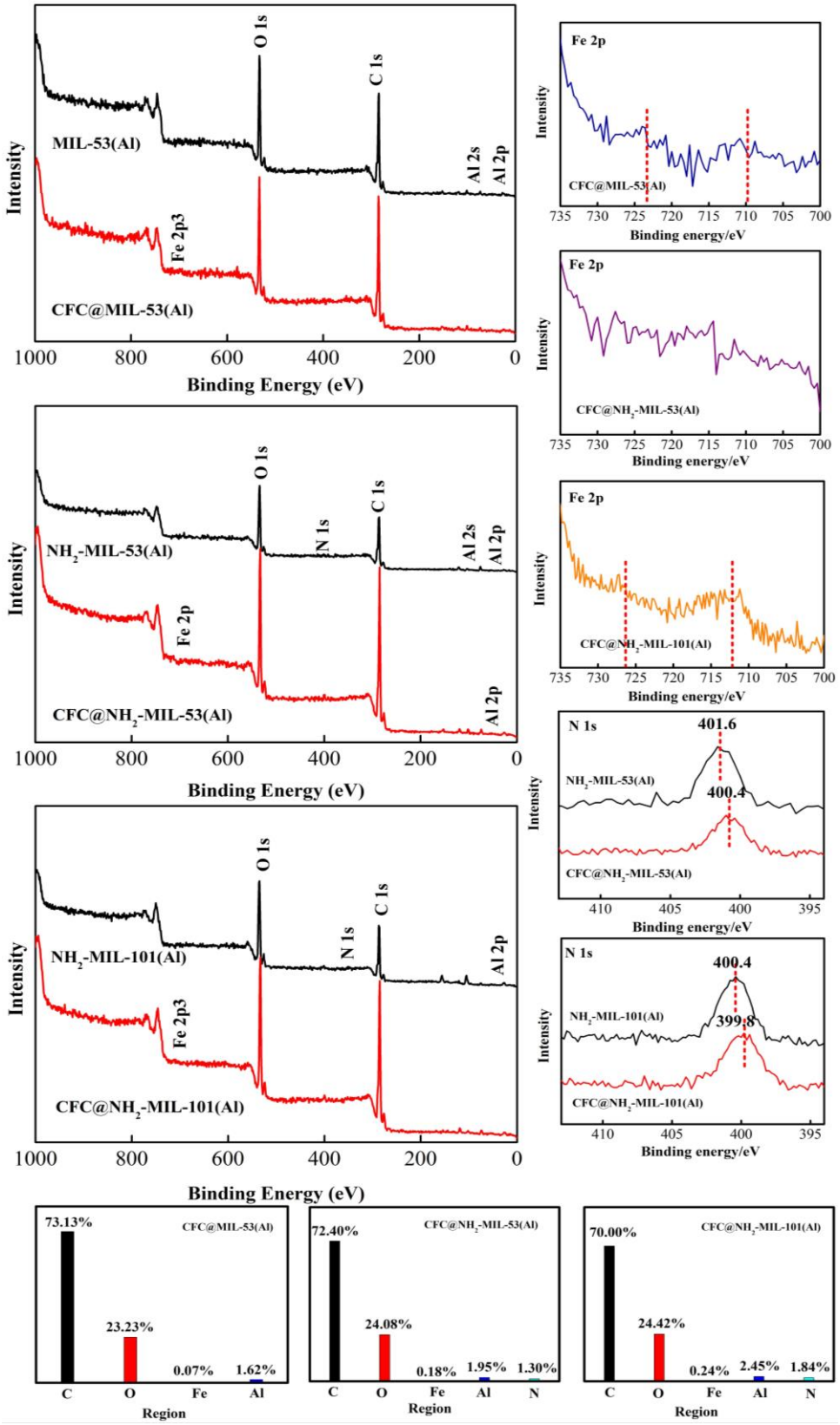

Figure S7 XPS spectra of different samples.

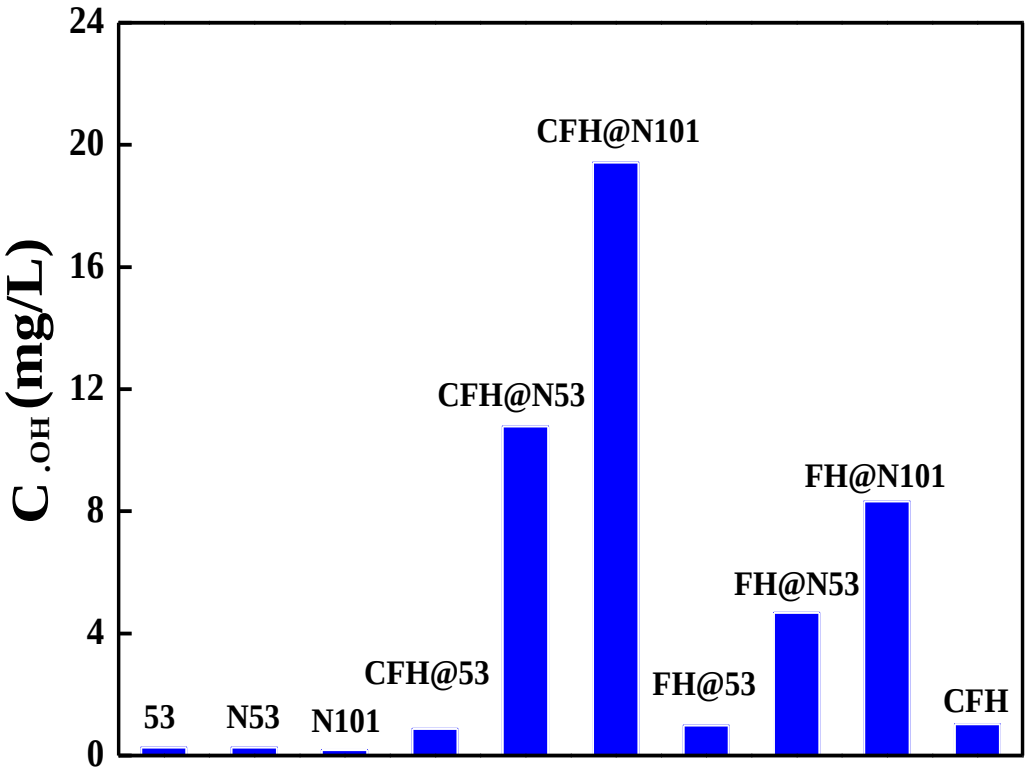

Figure S8 Concentration of •OH radicals in the oxidation system with different catalysts.

To better explore the influence of introduction of CA on activity of the catalysts, we also prepared FH@NH_2-MIL-53 or NH_2-MIL-101 and investigated their photocatalytic ability. After Fe-only loading treatment, an evident reduction in the production of OH was observed for these two samples. It was surprisingly found that the leaching content of Fe ions for both samples was over 0.60 mg L^{-1}, several times larger than that with CA adding. It well confirmed that the addition of CA can not only greatly improved catalytic activity for splitting of H_2O_2, but also provided strong binding force between metallic site and free amine moiety on Al-based MOFs.

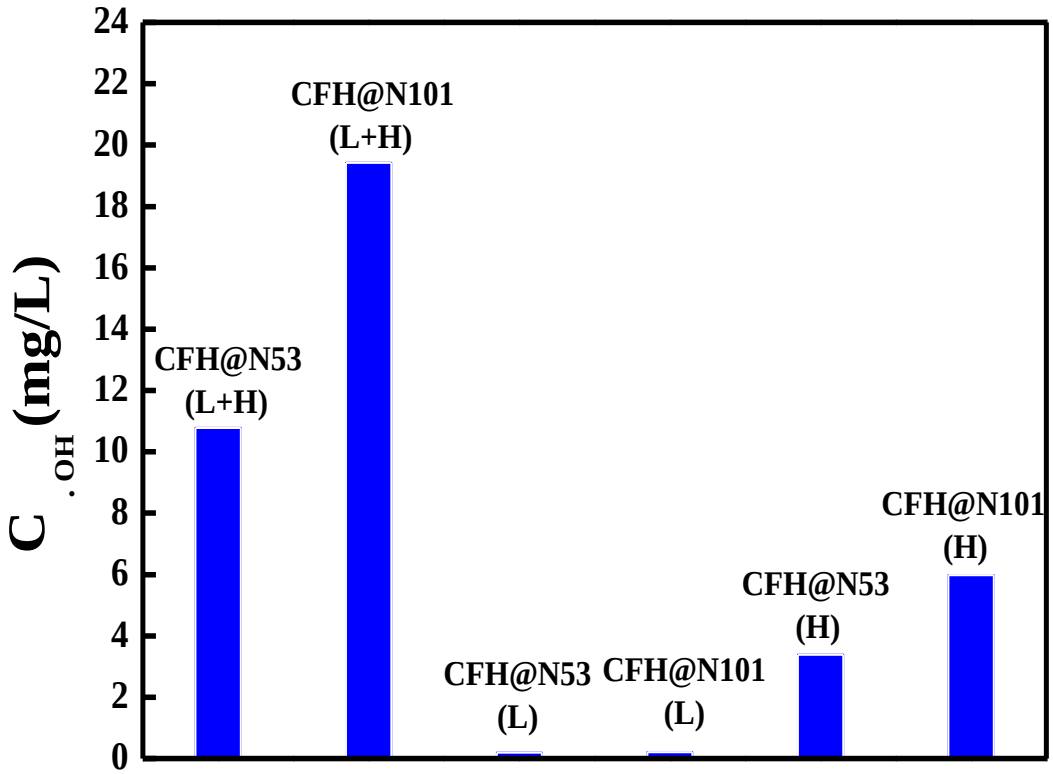

Figure S9 Concentration of ·OH with different conditions and catalysts (L= visible light; H= H_2O_2).

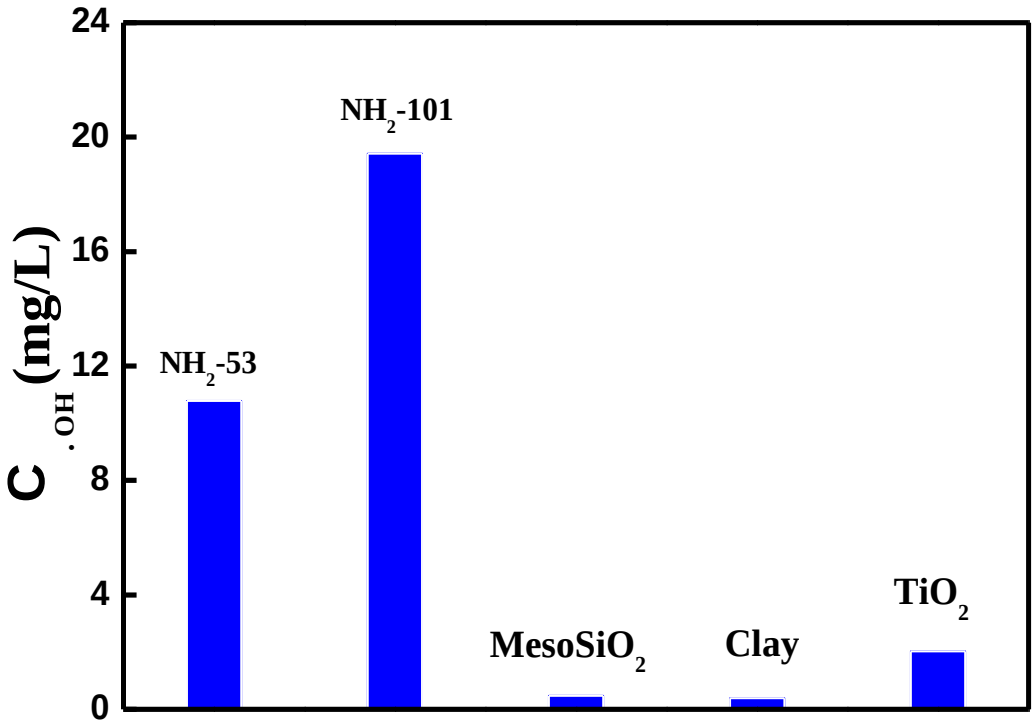

Figure S10 Effect of the different supports decorated with Fe-C oxides NPs on the generation of ·OH.

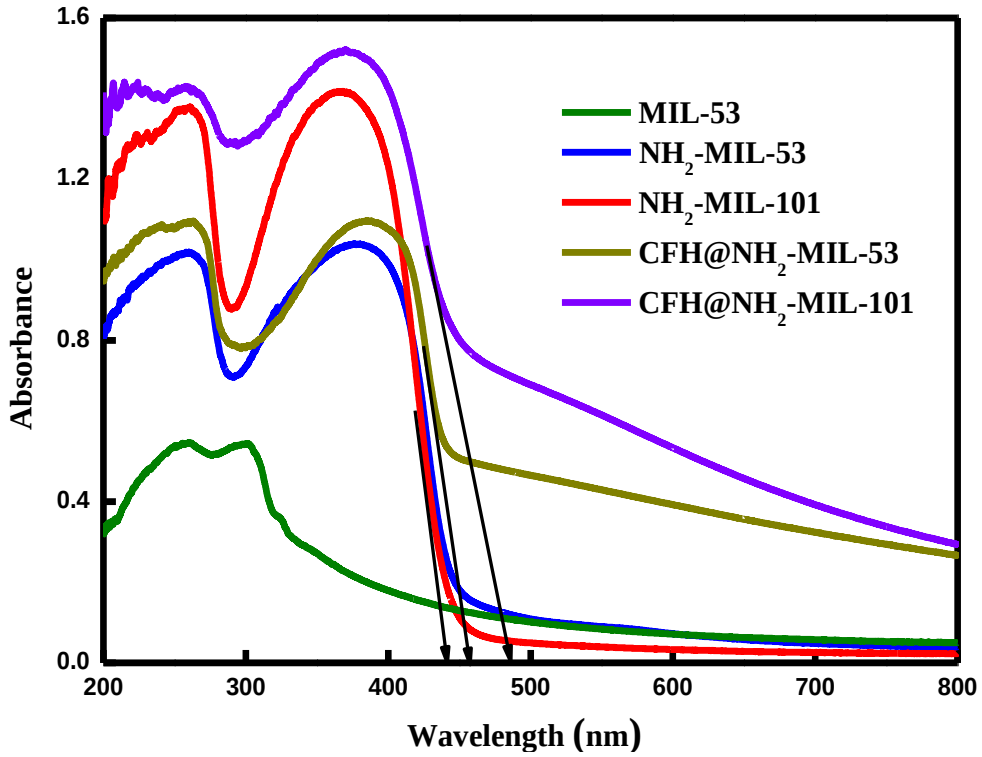

Figure S11 UV−visible diffuse reflectance spectra of the different prepared samples.

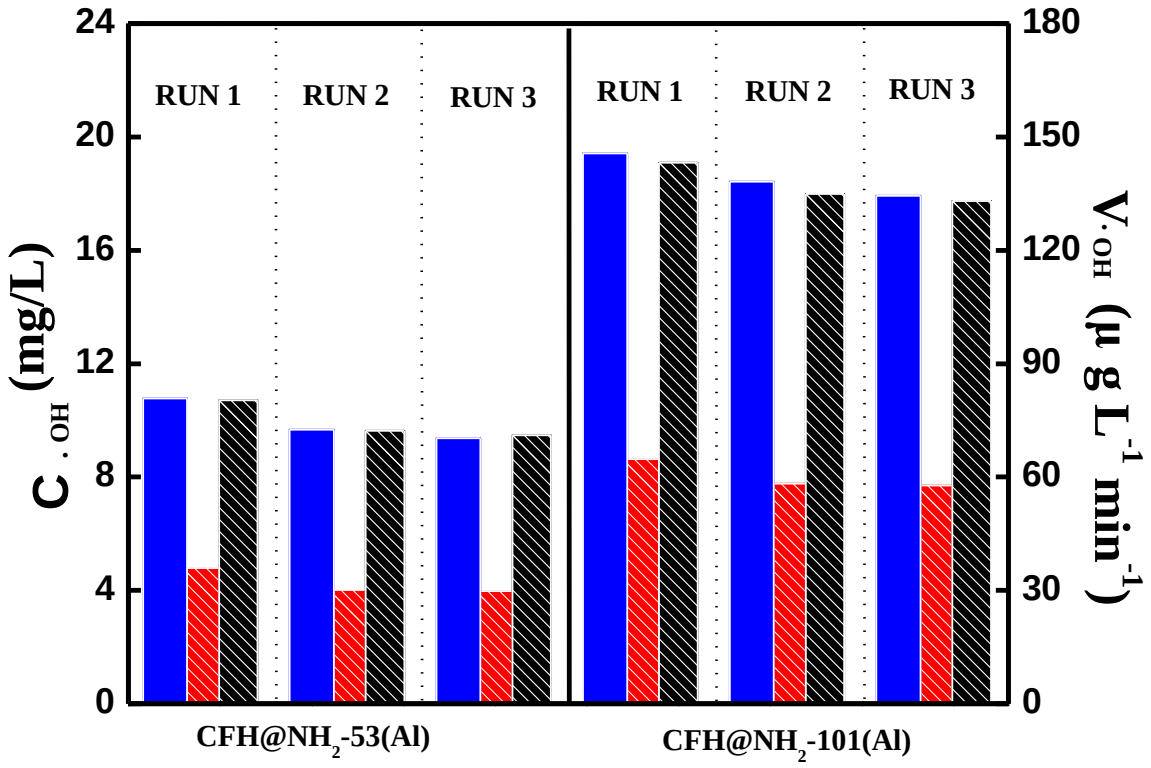

Figure S12 Reusability of the CFH@MIL-53 (a) and CFH@MIL-101 (b) after subsequent reactions (concentration (blue for 5 h) and generation rate (black for 0.5 h and red for 5 h) of •OH radicals).

During three catalytic runs, no significant loss in activity was presented for sample NH_2-MIL-101 and NH_2-MIL-53 after careful washings with methanol and drying (Fig. S12 ESI†). XRD and FTIR analysis reveals that the crystalline structure and surface properties of MOFs were not destroyed after photocatalytic splitting (Fig. S13 ESI†). TEM images also pointed out NPs uniformly deposited inside MOFs by multiple uses in catalysis, which demonstrates that the covalent bonding between amine groups and Fe-CA complex made catalysts intensely oppose photo-corrosion (Fig. S14 ESI†).

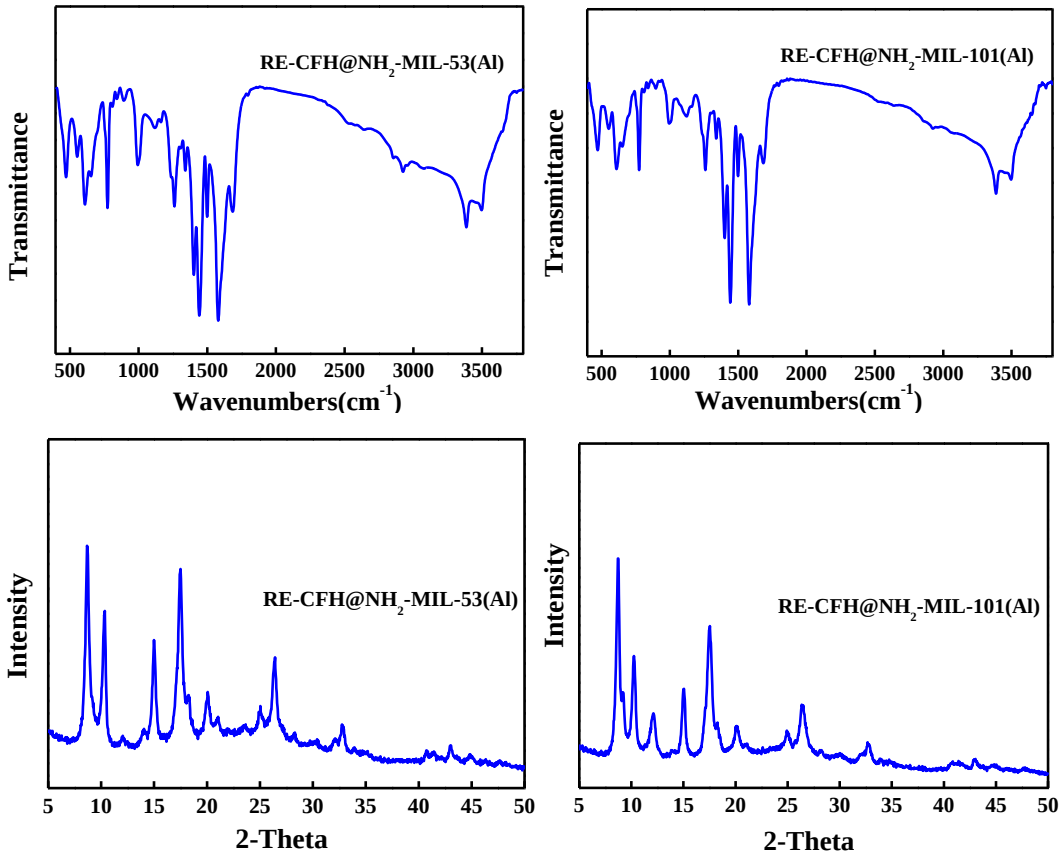

Figure S13 FTIR and XRD spectrums of the samples reused.

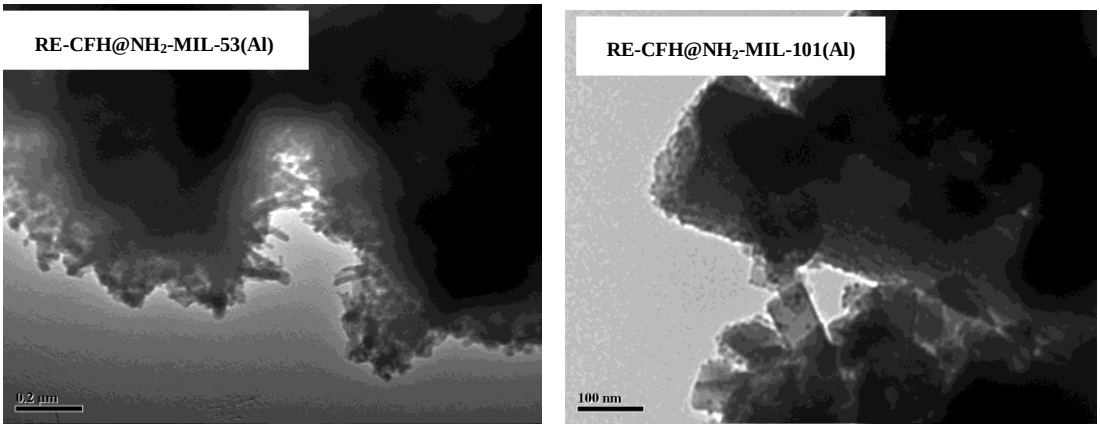

Figure S14 TEM investigations of the reused samples.